

LEGENDRIAN HOPF LINKS IN $L(p, 1)$

RIMA CHATTERJEE, HANSJÖRG GEIGES, AND SINEM ONARAN

ABSTRACT. We classify Legendrian realisations, up to coarse equivalence, of the Hopf link in the lens spaces $L(p, 1)$ with any contact structure.

1. INTRODUCTION

By the (positive) *Hopf link* $L_0 \sqcup L_1$ in the lens space $L(p, 1)$ we mean the (ordered, oriented) link formed by the two rational unknots given by the spines of the genus 1 Heegaard decomposition, oriented in such a way that their rational linking number equals $1/p$. By the discussion in [6, Section 2], this characterisation determines the link up to isotopy and a simultaneous change of orientations (which can be effected by an orientation-preserving diffeomorphism of $L(p, 1)$); the key result in the background is the uniqueness of the genus 1 Heegaard splitting up to isotopy.

The lens space $L(p, 1)$ with its natural orientation as a quotient of S^3 can be realised by a single $(-p)$ -surgery on an unknot. The Hopf link in this surgery diagram is shown in Figure 1; the link is positive when both L_0 and L_1 are oriented as meridians of the surgery curve in the same way. Indeed, if we label meridian and longitude (given by the Seifert framing) of the surgery curve by μ and λ , the $(-p)$ -surgery amounts to replacing a tubular neighbourhood of the surgery curve by a solid torus $V_1 = S^1 \times D^2$, with meridian $\mu_1 = \{*\} \times \partial D^2$ and longitude $\lambda_1 = S^1 \times \{1\}$ glued as follows:

$$\mu_1 \longmapsto p\mu - \lambda, \quad \lambda_1 \longmapsto \mu.$$

Then $L_1 = \mu = \lambda_1$ may be thought of as the spine of V_1 , and L_0 as the spine of the complementary solid torus V_0 , with meridian $\mu_0 = \lambda$ and longitude $\lambda_0 = \mu$.

A Seifert surface Σ_0 for pL_0 is made up of the radial surface in V_0 between the p -fold covered spine pL_0 and the curve

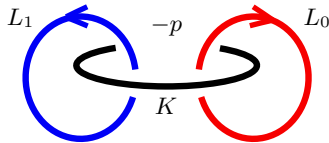
$$p\lambda_0 - \mu_0 = p\mu - \lambda = \mu_1,$$

and a (positively oriented) meridional disc in V_1 . The spine L_1 intersects this disc positively in a single point.

In this paper we extend the classification of Legendrian Hopf links in S^3 , see [7], to Legendrian Hopf links in $L(p, 1)$ for any $p \in \mathbb{N}$, with any contact structure. For a brief survey of the rather scant known results on the classification of Legendrian links (with at least two components) we refer to [7]. Our result is the first classification of Legendrian links in a 3-manifold other than S^3 .

2020 *Mathematics Subject Classification.* 57K33, 57K10, 57K40, 57R25.

R. C. and H. G. are partially supported by the SFB/TRR 191 ‘Symplectic Structures in Geometry, Algebra and Dynamics’, funded by the DFG (Project-ID 281071066 - TRR 191); S. O. is partially supported by TÜBİTAK Grant No. 119F411. R. C. and S. O. would like to thank the Max Planck Institute for Mathematics in Bonn for its hospitality.

FIGURE 1. The positive Hopf link in $L(p, 1)$.

Legendrian links in overtwisted contact manifolds are either *loose* (the link complement is still overtwisted) or *exceptional* (the link complement is tight). In the exceptional case, the link complement may or may not contain Giroux torsion. In contrast with [7], we only consider the case of vanishing Giroux torsion (what in [7] we called *strongly exceptional*); the case of Giroux torsion adds numerical complexity but no significant insight. Beware that the individual components of an exceptional Legendrian link may well be loose.

Our classification of the Legendrian realisations (up to coarse equivalence, i.e. up to a contactomorphism of the ambient manifold) of the Hopf link in $L(p, 1)$ is in terms of the rational classical invariants as defined in [1].

Lemma 1.1. *The rational Thurston–Bennequin invariant of the L_i , in any contact structure on $L(p, 1)$, is of the form $\text{tb}_{\mathbb{Q}}(L_i) = \mathfrak{t}_i + \frac{1}{p}$ with $\mathfrak{t}_i \in \mathbb{Z}$.*

Proof. By symmetry it suffices to show this for L_0 , where we can use the above description of a Seifert surface Σ_0 for pL_0 . The contact framing of L_0 is given by a curve $\mathfrak{t}_0\mu_0 + \lambda_0$ with $\mathfrak{t}_0 \in \mathbb{Z}$. With the identifications in the surgery description of $L(p, 1)$ we have

$$\mathfrak{t}_0\mu_0 + \lambda_0 = \mathfrak{t}_0\lambda + \mu = \mathfrak{t}_0(p\lambda_1 - \mu_1) + \lambda_1.$$

We can push this curve on ∂V_1 a little into V_1 , and then the intersection number with the meridional disc bounded by μ_1 (as part of Σ_0) equals $\mathfrak{t}_0p + 1$. To obtain $\text{tb}_{\mathbb{Q}}(L_0)$, this number has to be divided by p . \square

The rational rotation number $\text{rot}_{\mathbb{Q}}$ is well defined (i.e. independent of a choice of rational Seifert surface), since the Euler class of any contact structure on $L(p, 1)$ is a torsion class.

We also include the d_3 -invariant of the overtwisted contact structures. This invariant does not play a direct role in the classification, but in some cases we need it to determine whether the link components are loose or exceptional, when we appeal to the classification of exceptional Legendrian rational unknots in $L(p, 1)$ achieved in [6]. The notation ξ_d stands for an overtwisted contact structure with $d_3 = d$. For a complete homotopical classification of the overtwisted contact structures one also needs to know their Euler class (or, in the presence of 2-torsion, a finer d_2 -invariant). The Euler class can be computed from the surgery diagrams we present, using the recipe of [2]. These computations, which are rather involved, are omitted here. In the cases where we use contact cuts to find the Legendrian realisations, the homotopical classification of the contact structure in question is more straightforward.

We use the notation ξ_{tight} for any one of the tight contact structures on $L(p, 1)$. The homotopical data of the relevant contact structures containing Legendrian realisations of the Hopf link can easily be read off from Figure 2. These tight structures are Stein fillable and hence have zero Giroux torsion.

The essence of the following main theorem is that the classical invariants suffice to classify the Legendrian realisations of the Hopf link in $L(p, 1)$, so the Hopf link is what is called Legendrian simple.

Theorem 1.2. *Up to coarse equivalence, the Legendrian realisations of the Hopf link in $L(p, 1)$, $p \geq 2$, with zero Giroux torsion in the complement, are as follows. In all cases, the classical invariants determine the Legendrian realisation.*

- (a) *In $(L(p, 1), \xi_{\text{tight}})$ there is a unique realisation for any combination of classical invariants $(\text{tb}_{\mathbb{Q}}(L_i), \text{rot}_{\mathbb{Q}}(L_i)) = (\mathfrak{t}_i + \frac{1}{p}, \mathfrak{r}_i - \frac{\mathfrak{r}}{p})$, $i = 0, 1$, in the range $\mathfrak{t}_0, \mathfrak{t}_1 < 0$ and*

$$\mathfrak{r} \in \{-p+2, -p+4, \dots, p-4, p-2\},$$

$$\mathfrak{r}_i \in \{\mathfrak{t}_i + 1, \mathfrak{t}_i + 3, \dots, -\mathfrak{t}_i - 3, -\mathfrak{t}_i - 1\}.$$

For fixed values of $\mathfrak{t}_0, \mathfrak{t}_1 < 0$ this gives a total of $\mathfrak{t}_0 \mathfrak{t}_1 (p-1)$ realisations.

- (b) *For $\mathfrak{t}_0 = 0$ and $\mathfrak{t}_1 \leq 0$ there are $|\mathfrak{t}_1 - 1|$ exceptional realisations, all living in $(L(p, 1), \xi_d)$ with $d = (3-p)/4$, made up of an exceptional component L_0 with classical invariants $(\text{tb}_{\mathbb{Q}}(L_0), \text{rot}_{\mathbb{Q}}(L_0)) = (\frac{1}{p}, 0)$, and a loose component L_1 with invariants $(\text{tb}_{\mathbb{Q}}(L_1), \text{rot}_{\mathbb{Q}}(L_1)) = (\mathfrak{t}_1 + \frac{1}{p}, \mathfrak{r}_1)$, where*

$$\mathfrak{r}_1 \in \{\mathfrak{t}_1, \mathfrak{t}_1 + 2, \dots, -\mathfrak{t}_1 - 2, -\mathfrak{t}_1\}.$$

- (c) *For $\mathfrak{t}_0 = 0$ and $\mathfrak{t}_1 > 0$ the exceptional realisations are as follows; in all cases both components are loose.*
(c1) *For $\mathfrak{t}_1 = 1$ there are two realisations, with classical invariants*

$$(\text{tb}_{\mathbb{Q}}(L_0), \text{rot}_{\mathbb{Q}}(L_0)) = \left(\frac{1}{p}, \pm \frac{2}{p}\right)$$

and

$$(\text{tb}_{\mathbb{Q}}(L_1), \text{rot}_{\mathbb{Q}}(L_1)) = \left(1 + \frac{1}{p}, \pm \left(1 + \frac{2}{p}\right)\right).$$

They live in $(L(p, 1), \xi_d)$ with $d = (3p - p^2 - 4)/4p$.

- (c2) *For $\mathfrak{t}_1 = 2$, there are three exceptional realisations. Two of them live in $(L(p, 1), \xi_d)$, where $d = \frac{3p - p^2 - 4}{4p}$, and have classical invariants $(\text{tb}_{\mathbb{Q}}(L_0), \text{rot}_{\mathbb{Q}}(L_0))$ as in (c1) and*

$$(\text{tb}_{\mathbb{Q}}(L_1), \text{rot}_{\mathbb{Q}}(L_1)) = \left(2 + \frac{1}{p}, \pm \left(2 + \frac{2}{p}\right)\right).$$

The third one lives in $(L(p, 1), \xi_d)$ with $d = \frac{7-p}{4}$, and the invariants are $(\text{tb}_{\mathbb{Q}}(L_0), \text{rot}_{\mathbb{Q}}(L_0)) = (\frac{1}{p}, 0)$ and $(\text{tb}_{\mathbb{Q}}(L_1), \text{rot}_{\mathbb{Q}}(L_1)) = (2 + \frac{1}{p}, 0)$.

- (c3) *For $\mathfrak{t}_1 > 2$, there are four exceptional realisations. The classical invariants are listed in Table 1 in Section 7.*

- (d) *For $\mathfrak{t}_0, \mathfrak{t}_1 > 0$ the exceptional realisations, with both components loose, are as follows:*

- (d1) *For $\mathfrak{t}_0 = \mathfrak{t}_1 = 1$, there are exactly $p+3$ exceptional realisations. They live in $(L(p, 1), \xi_d)$, where $d = \frac{7p - \mathfrak{r}^2}{4p}$. They have classical invariants*

$$(\text{tb}_{\mathbb{Q}}(L_0), \text{rot}_{\mathbb{Q}}(L_0)) = \left(1 + \frac{1}{p}, \frac{\mathfrak{r}}{p}\right)$$

and

$$(\mathbf{tb}_{\mathbb{Q}}(L_1), \mathbf{rot}_{\mathbb{Q}}(L_1)) = \left(1 + \frac{1}{p}, \frac{\mathbf{r}}{p}\right),$$

where

$$\mathbf{r} \in \{-p-2, -p, \dots, p, p+2\}.$$

- (d2) For $\mathbf{t}_0 = 1$ and $\mathbf{t}_1 > 1$, there are $2(p+2)$ exceptional realisations, whose classical invariants are given in Table 2.
- (d3) For $\mathbf{t}_0 > 1$ and $\mathbf{t}_1 > 1$, there are $4(p+1)$ exceptional realisations, whose classical invariants are given in Table 3.
- (e) For $\mathbf{t}_0 < 0$ and $\mathbf{t}_1 > 0$ the exceptional realisations are as follows. Here L_0 is loose; L_1 is exceptional.
 - (e1) For $\mathbf{t}_1 = 1$, there are exactly $|\mathbf{t}_0|(p+1)$ exceptional realisations. They live in $(L(p, 1), \xi_d)$ where $d = (3p - \mathbf{r}^2)/4p$, where

$$\mathbf{r} \in \{-p, -p+2, \dots, p-2, p\}.$$

The classical invariants are

$$(\mathbf{tb}_{\mathbb{Q}}(L_0), \mathbf{rot}_{\mathbb{Q}}(L_0)) = \left(\mathbf{t}_0 + \frac{1}{p}, \mathbf{r}_0 - \frac{\mathbf{r}}{p}\right)$$

and

$$(\mathbf{tb}_{\mathbb{Q}}(L_1), \mathbf{rot}_{\mathbb{Q}}(L_1)) = \left(1 + \frac{1}{p}, -\frac{\mathbf{r}}{p}\right),$$

where

$$\mathbf{r}_0 \in \{\mathbf{t}_0 + 1, \mathbf{t}_0 + 3, \dots, -\mathbf{t}_0 - 3, -\mathbf{t}_0 - 1\}.$$

- (e2) For $\mathbf{t}_0 < 0$ and $\mathbf{t}_1 > 1$, there are $2|\mathbf{t}_0|p$ exceptional realisations, whose classical invariants are given in Section 7.2.7.

The proof of Theorem 1.2 largely follows the strategy used in [7] for Legendrian Hopf links in S^3 : find an upper bound on the number of exceptional realisations by enumerating the tight contact structures on the link complement, and then show that this bound is attained by giving explicit realisations.

Most of these explicit realisations are in terms of surgery diagrams, but as in [7] there is a case where a surgery presentation eludes us, and we have to use contact cuts instead. This case (c1), which is being treated in Section 5, contains most of the conceptually novel aspects in the present paper. In contrast with [7], we no longer have a global frame for the contact structure; therefore, the computation of rotation numbers requires the explicit description of rational Seifert surfaces, and frames over them, in the context of topological cuts. The discussion in Section 5 should prove useful in a more general analysis of the contact topology of lens spaces via contact cuts.

Remark 1.3. One has to be a little careful when comparing this result with the classification of Legendrian Hopf links in S^3 in [7]. For instance, in case (c1), the contact cut description we use in Section 5 corresponds for $p = 1$ to the interpretation of S^3 as lens space $L(1, 1)$, whereas in [7] we read S^3 as $L(1, 0)$. In case (a), the surgery diagram for S^3 is empty, and the discussion in the present paper only makes sense for $p \geq 2$. In most other cases, however, one obtains the correct results for S^3 by allowing $p = 1$ in Theorem 1.2.

2. UPPER BOUND FOR EXCEPTIONAL REALISATIONS

In this section we determine the number of tight contact structures on the complement of a Legendrian Hopf link $L_0 \sqcup L_1$ in $L(p, 1)$, in terms of the Thurston–Bennequin invariant of the link components. We start with S^3 , decomposed into two solid tori V_0, V_1 forming a Hopf link (in the traditional sense), and a thickened torus $T^2 \times [0, 1]$, i.e.

$$S^3 = V_0 \cup_{\partial V_0 = T^2 \times \{0\}} T^2 \times [0, 1] \cup_{T^2 \times \{1\} = \partial V_1} V_1.$$

Write μ_i, λ_i for meridian and longitude on ∂V_i , and define the gluing in the decomposition above by

$$\begin{aligned} \mu_0 &= S^1 \times \{*\} \times \{0\}, \\ \lambda_0 &= \{*\} \times S^1 \times \{0\}, \\ \mu_1 &= \{*\} \times S^1 \times \{1\}, \\ \lambda_1 &= S^1 \times \{*\} \times \{1\}. \end{aligned}$$

As in the introduction, we think of the Hopf link in $L(p, 1)$ as being obtained by $(-p)$ -surgery along the spine of V_1 . Slightly changing the notation from the introduction, we write μ'_1, λ'_1 for meridian and longitude of the solid torus V'_1 reglued in place of V_1 , so that the gluing prescription becomes

$$\mu'_1 \mapsto p\mu_1 - \lambda_1, \quad \lambda'_1 \mapsto \mu_1.$$

Given a Legendrian Hopf link $L_0 \sqcup L_1$ in $L(p, 1)$ with $\text{tb}_{\mathbb{Q}}(L_i) = \mathfrak{t}_i + \frac{1}{p}$, we can choose V_0, V'_1 (*sic!*) as standard neighbourhoods of L_0, L_1 , respectively. This means that ∂V_0 is a convex surface with two dividing curves of slope $1/\mathfrak{t}_0$ with respect to (μ_0, λ_0) ; the slope of $\partial V'_1$ is $1/\mathfrak{t}_1$ with respect to (μ'_1, λ'_1) .

Now, on $T^2 \times [0, 1]$ we measure slopes on the T^2 -factor with respect to (μ_0, λ_0) . So we are dealing with a contact structure on $T^2 \times [0, 1]$ with convex boundary, two dividing curves on either boundary component, of slope $s_0 = 1/\mathfrak{t}_0$ on $T^2 \times \{0\}$, and of slope $s_1 = -p - 1/\mathfrak{t}_1$ on $T^2 \times \{1\}$, since

$$\mathfrak{t}_1 \mu'_1 + \lambda'_1 = \mathfrak{t}_1(p\mu_1 - \lambda_1) + \lambda_1 = (\mathfrak{t}_1 p + 1)\lambda_0 - \mathfrak{t}_1 \mu_0.$$

Recall that a contact structure on $T^2 \times [0, 1]$ with these boundary conditions is called *minimally twisting* if every convex torus parallel to the boundary has slope between s_1 and s_0 .

The following proposition covers all possible pairs $(\mathfrak{t}_0, \mathfrak{t}_1)$, possibly after exchanging the roles of L_0 and L_1 .

Proposition 2.1. *Up to an isotopy fixing the boundary, the number $N = N(\mathfrak{t}_0, \mathfrak{t}_1)$ of tight, minimally twisting contact structures on $T^2 \times [0, 1]$ with convex boundary, two dividing curves on either boundary component of slope $s_0 = 1/\mathfrak{t}_0$ and $s_1 = -p - 1/\mathfrak{t}_1$, respectively, is as follows.*

- (a) If $\mathfrak{t}_0, \mathfrak{t}_1 < 0$, we have $N = \mathfrak{t}_0 \mathfrak{t}_1 (p - 1)$.
- (b) If $\mathfrak{t}_0 = 0$ and $\mathfrak{t}_1 \leq 0$, then $N = |\mathfrak{t}_1 - 1|$.
- (c) If $\mathfrak{t}_0 = 0, \mathfrak{t}_1 \geq 1$:
 - (c1) $N(0, 1) = 2$.
 - (c2) $N(0, 2) = 3$.
 - (c3) For all $\mathfrak{t}_1 > 2$, we have $N(0, \mathfrak{t}_1) = 4$.
- (d) If $\mathfrak{t}_0, \mathfrak{t}_1 > 0$:
 - (d1) $N(1, 1) = p + 3$.

- (d2) For all $\mathfrak{t}_1 > 1$, we have $N(1, \mathfrak{t}_1) = 2(p+2)$.
- (d3) For all $\mathfrak{t}_0, \mathfrak{t}_1 > 1$, we have $N = 4(p+1)$.
- (e) If $\mathfrak{t}_0 < 0, \mathfrak{t}_1 > 0$:
 - (e1) For all $\mathfrak{t}_0 < 0$ and $\mathfrak{t}_1 > 1$, we have $N = 2|\mathfrak{t}_0|p$.
 - (e2) For all $\mathfrak{t}_0 < 0$, we have $N(\mathfrak{t}_0, 1) = |\mathfrak{t}_0|(p+1)$.

Proof. So that we can use the classification of tight contact structures on $T^2 \times [0, 1]$ due to Giroux [8] and Honda [9], we normalise the slopes by applying an element of $\text{Diff}^+(T^2) \cong \text{SL}(2, \mathbb{Z})$ to $T^2 \times [0, 1]$ such that the slope on $T^2 \times \{0\}$ becomes $s'_0 = -1$, and on $T^2 \times \{1\}$ we have $s'_1 \leq -1$. If $s'_1 < -1$, the number N is found from a continuous fraction expansion

$$s'_1 = r_0 - \frac{1}{r_1 - \frac{1}{r_2 - \cdots - \frac{1}{r_k}}} =: [r_0, \dots, r_k]$$

with all $r_i < -1$ as

$$(1) \quad N = |(r_0 + 1) \cdots (r_{k-1} + 1)r_k|,$$

see [9, Theorem 2.2(2)]. The vector $\begin{pmatrix} x \\ y \end{pmatrix}$ stands for the curve $x\mu_0 + y\lambda_0$, with slope y/x .

2.1. Case (a). We have

$$\begin{pmatrix} 0 & -1 \\ 1 & -\mathfrak{t}_0 + 1 \end{pmatrix} \begin{pmatrix} \mathfrak{t}_0 \\ 1 \end{pmatrix} = \begin{pmatrix} -1 \\ 1 \end{pmatrix}$$

and

$$\begin{pmatrix} 0 & -1 \\ 1 & -\mathfrak{t}_0 + 1 \end{pmatrix} \begin{pmatrix} -\mathfrak{t}_1 \\ p\mathfrak{t}_1 + 1 \end{pmatrix} = \begin{pmatrix} -p\mathfrak{t}_1 - 1 \\ -\mathfrak{t}_1 - p\mathfrak{t}_0\mathfrak{t}_1 + p\mathfrak{t}_1 - \mathfrak{t}_0 + 1 \end{pmatrix},$$

which implies

$$s'_1 = \mathfrak{t}_0 - 1 + \frac{\mathfrak{t}_1}{p\mathfrak{t}_1 + 1} = \mathfrak{t}_0 - 1 - \frac{1}{-p - \frac{1}{\mathfrak{t}_1}}.$$

For $\mathfrak{t}_1 < -1$ we read this as $[\mathfrak{t}_0 - 1, -p, \mathfrak{t}_1]$; for $\mathfrak{t}_1 = -1$ and $p > 2$, as $[\mathfrak{t}_0 - 1, -p + 1]$; for $\mathfrak{t}_1 = -1$ and $p = 2$, as $[\mathfrak{t}_0]$. In all three cases this gives $N = |\mathfrak{t}_0\mathfrak{t}_1(p - 1)|$.

2.2. Case (b). For $\mathfrak{t}_0 = 0$ and $\mathfrak{t}_1 \leq 0$ we use the transformation

$$\begin{pmatrix} -p & -1 \\ p+1 & 1 \end{pmatrix} \begin{pmatrix} 0 \\ 1 \end{pmatrix} = \begin{pmatrix} -1 \\ 1 \end{pmatrix}$$

and

$$\begin{pmatrix} -p & -1 \\ p+1 & 1 \end{pmatrix} \begin{pmatrix} -\mathfrak{t}_1 \\ p\mathfrak{t}_1 + 1 \end{pmatrix} = \begin{pmatrix} -1 \\ 1 - \mathfrak{t}_1 \end{pmatrix}.$$

This gives $s'_1 = -1 + \mathfrak{t}_1$, whence $N = |\mathfrak{t}_1 - 1|$.

2.3. **Case (c).** For $t_0 = 0$ and $t_1 \geq 2$ we have

$$\begin{pmatrix} -(p+1) & -1 \\ p+2 & 1 \end{pmatrix} \begin{pmatrix} 0 \\ 1 \end{pmatrix} = \begin{pmatrix} -1 \\ 1 \end{pmatrix}$$

and

$$\begin{pmatrix} -(p+1) & -1 \\ p+2 & 1 \end{pmatrix} \begin{pmatrix} -\mathfrak{t}_1 \\ p\mathfrak{t}_1 + 1 \end{pmatrix} = \begin{pmatrix} \mathfrak{t}_1 - 1 \\ -2\mathfrak{t}_1 + 1 \end{pmatrix}.$$

A continued fraction expansion for $s'_1 = (-2\mathfrak{t}_1 + 1)/(\mathfrak{t}_1 - 1)$ is given by

$$[-3, \underbrace{-2, -2, \dots, -2}_{\mathfrak{t}_1 - 2}].$$

Hence, for $\mathfrak{t}_1 > 2$ we get $N = |(-2)(-1) \cdots (-1)(-2)| = 4$; for $\mathfrak{t}_1 = 2$ we have $N = 3$.

For $\mathfrak{t}_1 = 1$ we work instead with the transformation

$$\begin{pmatrix} -2p & -1 \\ 1+2p & 1 \end{pmatrix} \begin{pmatrix} 0 \\ 1 \end{pmatrix} = \begin{pmatrix} -1 \\ 1 \end{pmatrix}$$

and

$$\begin{pmatrix} -2p & -1 \\ 1+2p & 1 \end{pmatrix} \begin{pmatrix} -1 \\ p+1 \end{pmatrix} = \begin{pmatrix} p-1 \\ -p \end{pmatrix},$$

which gives

$$s'_1 = -\frac{p}{p-1} = [-2, \underbrace{-2, -2, \dots, -2}_{p-1}],$$

whence $N = 2$.

2.4. **Case (d).** For $\mathfrak{t}_0 > 0$ and $\mathfrak{t}_1 > 0$ we compute

$$\begin{pmatrix} -p & -1 + p\mathfrak{t}_0 \\ 1+p & 1 - (1+p)\mathfrak{t}_0 \end{pmatrix} \begin{pmatrix} \mathfrak{t}_0 \\ 1 \end{pmatrix} = \begin{pmatrix} -1 \\ 1 \end{pmatrix}$$

and

$$\begin{pmatrix} -p & -1 + p\mathfrak{t}_0 \\ 1+p & 1 - (1+p)\mathfrak{t}_0 \end{pmatrix} \begin{pmatrix} -\mathfrak{t}_1 \\ p\mathfrak{t}_1 + 1 \end{pmatrix} = \begin{pmatrix} -1 + p\mathfrak{t}_0 + p^2\mathfrak{t}_0\mathfrak{t}_1 \\ 1 - \mathfrak{t}_0 - \mathfrak{t}_1 - p\mathfrak{t}_0 - p\mathfrak{t}_0\mathfrak{t}_1 - p^2\mathfrak{t}_0\mathfrak{t}_1 \end{pmatrix}.$$

Hence,

$$s'_1 = -1 - \frac{\mathfrak{t}_0 + \mathfrak{t}_1 + p\mathfrak{t}_0\mathfrak{t}_1}{-1 + p\mathfrak{t}_0 + p^2\mathfrak{t}_0\mathfrak{t}_1}.$$

For $\mathfrak{t}_0 = 1$, the continued fraction expansion is

$$s'_1 = [\underbrace{-2, -2, \dots, -2}_{p-1}, -(p+3), \underbrace{-2, -2, \dots, -2}_{\mathfrak{t}_1 - 1}].$$

Thus, $N = p+3$ for $\mathfrak{t}_1 = 1$, and $N = 2(p+2)$ for $\mathfrak{t}_1 > 1$.

For $\mathfrak{t}_0, \mathfrak{t}_1 > 1$ we have the continued fraction expansion

$$s'_1 = [\underbrace{-2, -2, \dots, -2}_{p-1}, -3, \underbrace{-2, -2, \dots, -2}_{\mathfrak{t}_0 - 2}, -(p+2), \underbrace{-2, -2, \dots, -2}_{\mathfrak{t}_1 - 1}],$$

whence $N = 4(p+1)$.

2.5. **Case (e).** For $\mathfrak{t}_0 < 0$ and $\mathfrak{t}_1 > 0$ we use the transformation

$$\begin{pmatrix} -1 & \mathfrak{t}_0 - 1 \\ 2 & 1 - 2\mathfrak{t}_0 \end{pmatrix} \begin{pmatrix} \mathfrak{t}_0 \\ 1 \end{pmatrix} = \begin{pmatrix} -1 \\ 1 \end{pmatrix}$$

and

$$\begin{pmatrix} -1 & \mathfrak{t}_0 - 1 \\ 2 & 1 - 2\mathfrak{t}_0 \end{pmatrix} \begin{pmatrix} -\mathfrak{t}_1 \\ p\mathfrak{t}_1 + 1 \end{pmatrix} = \begin{pmatrix} -1 + \mathfrak{t}_0 + \mathfrak{t}_1 - p\mathfrak{t}_1 + p\mathfrak{t}_0\mathfrak{t}_1 \\ 1 - 2\mathfrak{t}_0 - 2\mathfrak{t}_1 + p\mathfrak{t}_1 - 2p\mathfrak{t}_0\mathfrak{t}_1 \end{pmatrix}.$$

Then

$$s'_1 = -2 - \frac{1 + p\mathfrak{t}_1}{-1 + \mathfrak{t}_0 + \mathfrak{t}_1 - p\mathfrak{t}_1 + p\mathfrak{t}_0\mathfrak{t}_1} = [-2, \mathfrak{t}_0 - 1, -(p+1), \underbrace{-2, -2, \dots, -2}_{\mathfrak{t}_1 - 1}].$$

For $\mathfrak{t}_1 > 1$ this yields $N = 2|\mathfrak{t}_0|p$; for $\mathfrak{t}_1 = 1$ we get $N = |\mathfrak{t}_0|(p+1)$. \square

3. COMPUTING THE INVARIANTS FROM SURGERY DIAGRAM

Except for the case (c1) discussed in terms of contact cuts in Section 5, we are going to describe the Legendrian realisations of the Hopf link in $L(p, 1)$ as front projections of a Legendrian link in a contact surgery diagram for $(L(p, 1), \xi)$ involving only contact (± 1) -surgeries. Here we briefly recall how to compute the classical invariants from such a presentation; for more details see [7, Section 5.2].

Write M for the linking matrix of the surgery diagram, with the surgery knots K_1, \dots, K_n given auxiliary orientations, and $\mathbf{lk}(K_j, K_j)$ equal to the topological surgery framing. The extended linking matrix of a Legendrian knot L_i in this surgery presentation is

$$M_i = \left(\begin{array}{c|ccc} 0 & \mathbf{lk}(L_i, K_1) & \cdots & \mathbf{lk}(L_i, K_n) \\ \hline \mathbf{lk}(L_i, K_1) & & & \\ \vdots & & M & \\ \mathbf{lk}(L_i, K_n) & & & \end{array} \right).$$

3.1. Thurston–Bennequin invariant. Write \mathbf{tb}_i for the Thurston–Bennequin invariant of L_i as a Legendrian knot in (S^3, ξ_{st}) , that is, before performing the contact surgeries. Then, in the surgered contact manifold, one has

$$\mathbf{tb}_{\mathbb{Q}}(L_i) = \mathbf{tb}_i + \frac{\det M_i}{\det M}.$$

3.2. Rotation number. Write \mathbf{rot}_i for the rotation number of L_i before the surgery. With

$$\underline{\mathbf{rot}} := (\mathbf{rot}(K_1), \dots, \mathbf{rot}(K_n))$$

and

$$\underline{\mathbf{lk}}_i := (\mathbf{lk}(L_i, K_1), \dots, \mathbf{lk}(L_i, K_n))$$

we have

$$\mathbf{rot}_{\mathbb{Q}}(L_i) = \mathbf{rot}_i - \langle \underline{\mathbf{rot}}, M^{-1} \underline{\mathbf{lk}}_i \rangle.$$

3.3. The d_3 -invariant. The surgery diagram describes a 4-dimensional handlebody X with signature σ and Euler characteristic $\chi = 1 + n$. Let $c \in H^2(X)$ be the cohomology class determined by $c(\Sigma_j) = \text{rot}(K_j)$, where Σ_j is the oriented surface made up of a Seifert surface for K_j and the core disc of the corresponding handle. Write q for the number of contact $(+1)$ -surgeries.

Then the d_3 -invariant is given by the formula

$$d_3(\xi) = \frac{1}{4}(c^2 - 3\sigma - 2\chi) + q,$$

where c^2 is computed as follows: find the solution vector \mathbf{x} of the equation $M\mathbf{x} = \underline{\text{rot}}$; then $c^2 = \mathbf{x}^t M \mathbf{x} = \langle \mathbf{x}, \underline{\text{rot}} \rangle$.

The signature σ can be computed from the linking matrix corresponding to the surgery diagram; more efficiently, one can usually compute it using Kirby moves as described in [7, p. 1433].

4. HOPF LINKS IN TIGHT $L(p, 1)$

For given values of $\mathfrak{t}_0, \mathfrak{t}_1 < 0$, we have $\mathfrak{t}_0 \mathfrak{t}_1 (p - 1)$ explicit realisations in $(L(p, 1), \xi_{\text{tight}})$ as shown in Figure 2. Here the numbers k, k_i and ℓ, ℓ_i refer to the exterior cusps, so that the surgery curve K has $\mathfrak{tb} = -k - \ell + 1$ (and $\mathfrak{tb}_i = -k_i - \ell_i + 1$), and to obtain $L(p, 1)$ by a contact (-1) -surgery on K we need $k + \ell = p$. The \mathfrak{tb}_i can take any negative value. With L_0, L_1 both oriented clockwise, the Hopf link is positive, and in this case we have $\text{rot}_i = \ell_i - k_i$.

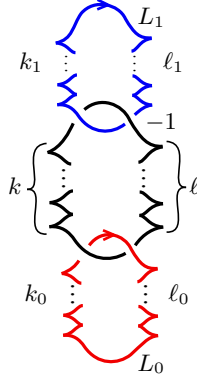


FIGURE 2. Legendrian Hopf links in $(L(p, 1), \xi_{\text{tight}})$. Here $k + \ell = p$.

The values of the classical invariants as claimed in Theorem 1.2 (a) now follow easily from the formulas in Section 3, with $\mathfrak{t}_i = \mathfrak{tb}_i$, $\mathfrak{r}_i = \text{rot}_i$, and $\mathfrak{r} = \text{rot}(K)$. For the d_3 -invariant we observe that $\sigma = -1$, $\chi = 2$, and $c^2 = -\mathfrak{r}^2/p$, whence

$$d_3 = -\frac{1}{4}\left(1 + \frac{\mathfrak{r}^2}{p}\right).$$

There are no realisations in $(L(p, 1), \xi_{\text{tight}})$ with one of the \mathfrak{t}_i being non-negative, since Legendrian rational unknots in $(L(p, 1), \xi_{\text{tight}})$ satisfy $\mathfrak{t}_i < 0$ by [1, Theorem 5.5] or [6, Theorem 7.1].

This proves part (a) of Theorem 1.2.

Remark 4.1. The values of the d_3 -invariant found above exhausts all possibilities for the d_3 -invariant of the tight contact structures on $L(p, 1)$; see [6, Section 4].

5. LEGENDRIAN HOPF LINKS VIA CONTACT CUTS

In this section we use contact cuts to find Legendrian realisations of Hopf links in $L(p, 1)$ for the case (c1).

5.1. $L(p, 1)$ as a cut manifold. We first want to give a topological description of $L(p, 1)$ as a cut manifold in the sense of Lerman [10]. We start from $T^2 \times [0, 1] = S^1 \times S^1 \times [0, 1]$ with coordinates $x, y \in S^1 = \mathbb{R}/\mathbb{Z}$ and $z \in [0, 1]$. Collapsing the first S^1 -factor in $S^1 \times S^1 \times \{0\}$ is equivalent to attaching a solid torus to $T^2 \times [0, 1]$ along $T^2 \times \{0\}$ by sending the meridian of the solid torus to $S^1 \times \{*\} \times \{0\}$. This, of course, simply amounts to attaching a collar to a solid torus, and the meridian of this ‘fattened’ torus is $\mu_0 := S^1 \times \{*\} \times \{1\}$. As longitude we take the curve $\lambda_0 := \{*\} \times S^1 \times \{1\}$.

Now, as described in Section 1, $L(p, 1)$ is obtained from this solid torus by attaching another solid torus, whose meridian is glued to the curve $p\lambda_0 - \mu_0$. Equivalently, we may collapse the foliation of $T^2 \times \{1\}$ by circles in the class $p\lambda_0 - \mu_0$.

Consider the p -fold cover $(\mathbb{R}/\mathbb{Z}) \times (\mathbb{R}/p\mathbb{Z}) \times [0, 1] \rightarrow (\mathbb{R}/\mathbb{Z}) \times (\mathbb{R}/\mathbb{Z}) \times [0, 1]$. Set $\tilde{\lambda}_0 := \{*\} \times (\mathbb{R}/p\mathbb{Z}) \times \{1\}$. The foliation of $(\mathbb{R}/\mathbb{Z}) \times (\mathbb{R}/p\mathbb{Z}) \times [0, 1]$ by circles in the class $\tilde{\lambda}_0 - \mu_0$ descends to the foliation defined by $p\lambda_0 - \mu_0$. This exhibits $L(p, 1)$ as a \mathbb{Z}_p -quotient of $L(1, 1) = S^3$. Beware that in [7] we used the description of S^3 as $L(1, 0)$ in the cut construction, so for $p = 1$ one has to take this into account when comparing the discussion here with the results in [7].

5.2. Contact structures from contact cuts. A contact structure on $T^2 \times [0, 1]$ will descend to the cut manifold $L(p, 1)$ if, at least near the boundary, it is invariant under the S^1 -action whose orbits on the boundary are collapsed to a point, and if the S^1 -action is tangent to the contact structure along the boundary.

We define $a \in (0, \pi/2)$ by the condition $\tan a = p$. For $\ell \in \mathbb{N}_0$, consider the contact form

$$\alpha_\ell := \sin((a + \ell\pi)z) dx + \cos((a + \ell\pi)z) dy$$

on $T^2 \times [0, 1]$. This 1-form is invariant under the flows of both ∂_x and ∂_y . Along $T^2 \times \{0\}$, we have $\partial_x \in \ker \alpha_\ell$; along $T^2 \times \{1\}$, the vector field $-\partial_x + p\partial_y$ is in $\ker \alpha_\ell$. Thus, α_ℓ descends to a contact form on $L(p, 1)$.

By [7, Proposition 6.1], adapted to the description of S^3 as $L(1, 1)$, the lift of $\ker \alpha_0$ to S^3 is the standard tight contact structure ξ_{st} . Indeed, the map $(x, y) \mapsto (x + y, y)$ sends this lifted contact structure on $T^2 \times [0, 1]$, up to isotopy rel boundary and compatibly with the cuts on the boundary, to the one shown in [7] to define ξ_{st} on $S^3 = L(1, 0)$.

This means that $\ker \alpha_0$ is the unique (up to diffeomorphism) universally tight contact structure on $L(p, 1)$. The contact structure $\ker \alpha_{\ell+1}$ is obtained from $\ker \alpha_\ell$ by a π -Lutz twist. In particular, $\ker \alpha_2$ is obtained from $\ker \alpha_0$ by a full Lutz twist, and hence is homotopically equivalent to the universally tight contact structure; see [5, Lemma 4.5.3]. The surgery description for the universally tight contact structure on $L(p, 1)$ is a contact (-1) -surgery on a $(p-2)$ -fold stabilised standard Legendrian unknot (with $\text{tb} = -1$ and $\text{rot} = 0$) in (S^3, ξ_{st}) , all stabilisations having the same sign. This contact structure has d_3 -invariant equal to $(3p - p^2 - 4)/4p$ and Euler class $\pm(p-2)$ (in terms of the natural cohomology generator); see [6, Section 4] and [4].

5.3. A Legendrian Hopf link in $(L(p, 1), \ker \alpha_2)$. The contact planes in $\ker \alpha_2$ on $T^2 \times [0, 1]$ have slope 0 with respect to (∂_x, ∂_y) at $z = 0$. As z increases to $z = 1$, the contact planes twist (with decreasing slope) for a little over 2π , until they reach slope $-p$ for the third time (and after passing through slope $\pm\infty$ twice), similar to Figure 18 in [7].

Define $z_0 < z_1$ in the interval $[0, 1]$ by the conditions

$$a + 2\pi z_0 = \frac{\pi}{2} \quad \text{and} \quad -\sin((a + 2\pi)z_1) + (p + 1)\cos((a + 2\pi)z_1) = 0.$$

This means that at $z = z_0$ the contact planes are vertical for the first time, and $T^2 \times \{z_1\}$ is the second torus (as z increases from 0 to 1) where the characteristic foliation has slope $-(p + 1)$.

Consider the link $L_0 \sqcup L_1$ made up of a $(0, 1)$ -curve on the torus $\{z = z_0\}$ and a $(-1, p + 1)$ -curve on $\{z = z_1\}$. This link is topologically isotopic to the one made up of a $(0, 1)$ -curve on $\{z = 0\}$ and a $(-1, p + 1)$ -curve on $\{z = 1\}$. Since these respective curves have intersection number ± 1 with the curves we collapse at either end,

$$(0, 1) \bullet (1, 0) = -1, \quad (-1, p + 1) \bullet (-1, p) = 1,$$

they are isotopic to the spine of the solid tori attached at either end, and so they constitute a Hopf link.

A Seifert surface Σ_0 for pL_0 , regarded as p times the spine of the solid torus attached at $z = 0$, is given by the following pieces:

- a helicoidal annulus between pL_0 and a $(-1, p)$ -curve on $\{z = 0\}$,
- an annulus between this $(-1, p)$ -curve on $\{z = 0\}$ and the same curve on $\{z = 1\}$,
- the meridional disc attached to the latter curve at $z = 1$.

Then

$$L_1 \bullet \Sigma_0 = (-1, p + 1) \bullet (-1, p) = -p + (p + 1) = 1.$$

Notice that ∂_y is positively transverse to Σ_0 on $T^2 \times [0, 1]$, so our calculation gives the correct sign of the intersection number. Thus, $L_0 \sqcup L_1$ is a *positive* Hopf link.

Both components L_0 and L_1 of this Legendrian Hopf link are loose, since the contact planes twist by more than π in either interval $(z_0, 1)$ and $(0, z_1)$, so the cut produces an overtwisted disc.

Lemma 5.1. *The Legendrian Hopf link $L_0 \sqcup L_1$ in $(L(p, 1), \ker \alpha_2)$ is exceptional.*

Proof. Arguing by contradiction, suppose there were an overtwisted disc in the complement of the link. This disc would persist in the complement of the transverse link $L'_0 \sqcup L'_1$ obtained by pushing L_0 a little towards $z = 0$, and L_1 towards $z = 1$. In $T^2 \times [0, 1]$, this link is transversely isotopic to the link made up of a $(0, 1)$ -curve on $\{z = 0\}$ and a $(-1, p + 1)$ -curve on $\{z = 1\}$. In the cut manifold $L(p, 1)$, this gives a transverse isotopy (and hence an ambient contact isotopy) from $L'_0 \sqcup L'_1$ to the transverse link made up of the collapsed boundaries $(T^2 \times \{0\})/S^1$ and $(T^2 \times \{1\})/S^1$. The complement of the latter, however, is contactomorphic to $(T^2 \times (0, 1), \ker \alpha_2)$, which is tight, as it embeds into the standard tight contact structure on \mathbb{R}^3 . \square

5.4. Computing $\mathbf{tb}_{\mathbb{Q}}$. A Legendrian push-off of L_0 is simply a parallel $(0, 1)$ -curve L'_0 on $\{z = z_0\}$. The topological isotopy from pL_0 to p times the spine of the solid torus attached at $z = 0$ can be performed in the complement of L'_0 . So the rational Thurston–Bennequin invariant (as defined in [1]) of L_0 is given by

$$\mathbf{tb}_{\mathbb{Q}}(L_0) = \frac{1}{p}L'_0 \bullet \Sigma_0 = \frac{1}{p}(0, 1) \bullet (-1, p) = \frac{1}{p}.$$

For L_1 we argue similarly. A Legendrian push-off L'_1 is given by a parallel $(-1, p+1)$ -curve on $\{z = z_1\}$. The isotopy of L_1 to the spine of the solid torus attached at $z = 1$ can be performed in the complement of L'_1 , so $\mathbf{tb}_{\mathbb{Q}}(L_1)$ can be computed as $L'_1 \bullet \Sigma_1$, where Σ_1 is a Seifert surface for p times that spine, made up of the following pieces:

- a helicoidal annulus between pL_1 and a curve on $\{z = 1\}$ in the class

$$p(-1, p+1) - (p+1)(-1, p) = (1, 0)$$

(see below for an explanation of this choice),

- an annulus between this $(1, 0)$ -curve on $\{z = 1\}$ and the same curve on $\{z = 0\}$,
- the meridional disc attached to the latter curve at $z = 0$.

For the first constituent of this Seifert surface, notice that the p -fold covered spine of a solid torus can be joined by an annulus to any simple curve on the boundary in a class $p\lambda + k\mu$, $k \in \mathbb{Z}$, where λ is any longitude on the boundary, and μ the meridian. Or, more directly, simply observe that in our case $\mu = (-1, p)$, and $(1, 0) \bullet (-1, p) = p$.

The vector field ∂_y is positively transverse to Σ_1 on $T^2 \times [0, 1]$, so we obtain

$$\mathbf{tb}_{\mathbb{Q}}(L_1) = \frac{1}{p}L'_1 \bullet \Sigma_1 = \frac{1}{p}(p+1) = 1 + \frac{1}{p}.$$

5.5. Frames for $\ker \alpha_{\ell}$. A frame for $\ker \alpha_{\ell}$ on $T^2 \times [0, 1]$, compatible with the orientation defined by $d\alpha_{\ell}$, is given by

$$\partial_z \quad \text{and} \quad X_{\ell} := \cos((a + \ell\pi)z)\partial_x - \sin((a + \ell\pi)z)\partial_y.$$

This frame does *not* descend to a frame of the contact structure on $L(p, 1)$.

At $z = 0$ we have $X_{\ell} = \partial_x$. If we think of the cut at $z = 0$ as being defined by attaching a solid torus, with meridian being sent to the x -curves, the vector field ∂_z is outward radial along the boundary of the solid torus, and $X_{\ell} = \partial_x$ is positively tangent to the meridional curves. It follows that a frame of $\ker \alpha_{\ell}$ that extends over the cut at $z = 0$ is given by

$$\cos(2\pi x)\partial_z - \sin(2\pi x)X_{\ell} \quad \text{and} \quad \sin(2\pi x)\partial_z + \cos(2\pi x)X_{\ell};$$

cf. [7, Figure 16].

At $z = 1$, where we collapse the flow lines of $-\partial_x + p\partial_y$, we have

$$X_{\ell} = \pm(\cos a \partial_x - \sin a \partial_y) = \mp \cos a (-\partial_x + p \partial_y),$$

depending on ℓ being even or odd. If we think of the cut again as attaching a solid torus, now ∂_z is inward radial along the boundary of the solid torus, and X_{ℓ} is tangent to the meridional curve (positively for ℓ odd, negatively for ℓ even). So the frame that extends over the cut at $z = 1$ is

$$\cos(2\pi x)\partial_z + \sin(2\pi x)X_{\ell} \quad \text{and} \quad -\sin(2\pi x)\partial_z + \cos(2\pi x)X_{\ell} \quad \text{for } \ell \text{ even,}$$

and

$$\cos(2\pi x)\partial_z - \sin(2\pi x)X_\ell \quad \text{and} \quad \sin(2\pi x)\partial_z + \cos(2\pi x)X_\ell \quad \text{for } \ell \text{ odd.}$$

Thus, only for ℓ odd do we have a global frame.

5.6. Computing $\text{rot}_{\mathbb{Q}}$. We now look again at the Legendrian Hopf link $L_0 \sqcup L_1$ in $(L(p, 1), \ker \alpha_2)$.

For the computation of the intersection number $L_1 \bullet \Sigma_0$ between L_1 and a Seifert surface for pL_0 we had the freedom to isotope L_0 (topologically) in the complement of L_1 to the spine of the solid torus attached at $z = 0$. When we want to compute $\text{rot}_{\mathbb{Q}}(L_0)$, we need to work with a Seifert surface for the original Legendrian L_0 . This means that we need to work with the Seifert surface Σ_0 made up of the following pieces:

- a p -fold covered straight annulus between pL_0 , i.e. the $(0, p)$ -curve on the torus $\{z = z_0\}$, and the p -fold covered spine of the solid torus attached at $z = 0$,
- a helicoidal annulus between p times the spine and a $(-1, p)$ -curve on the torus $\{z = 0\}$,
- an annulus between this $(-1, p)$ -curve on $\{z = 0\}$ and the same curve on $\{z = 1\}$,
- the meridional disc attached to the latter curve at $z = 1$.

Remark 5.2. This surface is not embedded, but the computation of rotation numbers is homological, so this is not a problem.

Our aim is to find a frame of $\ker \alpha_2$ defined over Σ_0 . We begin with the frame defined over $T^2 \times [0, 1]$ by $\cos(2\pi x)\partial_z + \sin(2\pi x)X_2$ (and its companion defining the correct orientation), which is the one that extends over the cut at $z = 1$. In particular, this frame is defined over the third and fourth constituent of Σ_0 , and we need to extend it over the first two pieces of Σ_0 .

Write $(\mathbb{R}/\mathbb{Z}) \times D^2$ with coordinates $(y; r, \theta)$ for the solid torus attached at $z = 0$. We pass to the p -fold covers

$$(\mathbb{R}/\mathbb{Z})^2 \times [0, 1] \longrightarrow (\mathbb{R}/\mathbb{Z})^2 \times [0, 1], \quad (x, y, z) \longmapsto (x, py, z)$$

and

$$(\mathbb{R}/\mathbb{Z}) \times D^2 \longrightarrow (\mathbb{R}/\mathbb{Z}) \times D^2, \quad (y; r, \theta) \longmapsto (py; r, \theta),$$

where the lifted pieces of Σ_0 are embedded: a straight annulus between the $(0, 1)$ -curve on $\{z = z_0\}$ and the spine of the solid torus, plus a helicoidal annulus between the spine and the $(-1, 1)$ -curve on the boundary of the solid torus. For the following homotopical considerations, we may think of $\ker \alpha_2$ as being extended over that solid torus as the constant horizontal plane field.

Along the $(-1, 1)$ curve on $\{z = 0\}$, parametrised as $\mathbb{R}/\mathbb{Z} \ni t \mapsto (x(t), y(t), 0) = (-t, t, 0)$, the frame we are considering is

$$\cos(2\pi t)\partial_z - \sin(2\pi t)\partial_x.$$

In the cylindrical coordinates $(y; r, \theta)$ on the solid torus this translates into the frame

$$\cos(2\pi t)\partial_r - \sin(2\pi t)\partial_\theta$$

along the curve $t \mapsto (y(t), \theta(t)) = (t, -2\pi t)$ on $\{r = 1\}$.

Next, we translate this into Cartesian coordinates (u, v) on the D^2 -factor. With $r\partial_r = u\partial_u + v\partial_v$ and $\partial_\theta = u\partial_v - v\partial_u$, and the curve in question being $(u(t), v(t)) = (\cos 2\pi t, -\sin 2\pi t)$, this gives the frame

$$\begin{aligned} & \cos(2\pi t)(\cos(2\pi t)\partial_u - \sin(2\pi t)\partial_v) - \\ & \sin(2\pi t)(\cos(2\pi t)\partial_v + \sin(2\pi t)\partial_u) = \cos(4\pi t)\partial_u - \sin(4\pi t)\partial_v. \end{aligned}$$

This formula defines the extension of the frame over the helicoidal annulus and the part of the straight annulus inside the solid torus. The intersection of the straight annulus with the torus $\{z = 0\}$ is the $(0, 1)$ -curve, parametrised as $t \mapsto (x(t), y(t)) = (0, t)$, and if we take this curve to be given by $\{u = 1, v = 0\}$ (so that $\partial_u = \partial_z$ and $\partial_v = \partial_x$), the frame is now written as

$$\cos(4\pi t)\partial_z - \sin(4\pi t)\partial_x,$$

which extends over the annulus between the $(0, 1)$ -curve on $\{z = 0\}$ and that on $\{z = z_0\}$ (i.e. the p -fold cover of L_0) as

$$\cos(4\pi t)\partial_z - \sin(4\pi t)X_2.$$

Notice that at $z = z_0$ we have $X_2 = -\partial_y$. The orientation of $\ker \alpha_2$ is defined by (∂_z, X_2) , so the frame makes two *negative* rotations with respect to the tangent vector $\partial_y = -X_2$ of the p -fold covered L_0 . We conclude that $\text{rot}_{\mathbb{Q}}(L_0) = 2/p$.

Next we compute $\text{rot}_{\mathbb{Q}}(L_1)$ in an analogous fashion. We now use the frame $\cos(2\pi x)\partial_z - \sin(2\pi x)X_2$ on $T^2 \times [0, 1]$, which is the one that extends over the cut at $z = 0$. The cut we perform at $z = 1$ corresponds to the attaching of a solid torus $(\mathbb{R}/\mathbb{Z}) \times D^2$ using the gluing map

$$\mu = \{0\} \times \partial D^2 \mapsto (-1, p) \quad \text{and} \quad \lambda = (\mathbb{R}/\mathbb{Z}) \times \{1\} \mapsto (-1, p+1).$$

Note that with respect to the orientation defined by (∂_x, ∂_y) , the intersection number of meridian and longitude is

$$\mu \bullet \lambda = (-1, p) \bullet (-1, p+1) = -1,$$

which is what we want, since ∂_z is the inward normal of the solid torus along its boundary, so this boundary is oriented by (∂_y, ∂_x) . Notice also that the tangent direction of μ coincides with $-X_2$.

The Legendrian knot L_1 on $\{z = z_1\}$ is a $(-1, p+1)$ -curve, so the parallel curve on $\{z = 1\}$ is in the class of λ . The relevant parts of the Seifert surface Σ_1 for pL_1 in the p -fold cover, i.e. the lift with respect to the map

$$(\mathbb{R}/\mathbb{Z}) \times D^2 \longrightarrow (\mathbb{R}/\mathbb{Z}) \times D^2, \quad (s; r, \theta) \longmapsto (ps; r, \theta),$$

are the following:

- a straight annulus between the lifted longitude and the spine,
 - a helicoidal annulus between the spine and the $(1, 0)$ -curve on $\{z = 1\}$;
- recall that $p\lambda - (p+1)\mu = (1, 0)$.

At $z = 1$, the frame $\cos(2\pi x)\partial_z - \sin(2\pi x)X_2$ we have chosen equals

$$\cos(2\pi x)\partial_z + \sin(2\pi x)\cos a(-\partial_x + p\partial_y).$$

Along the $(1, 0)$ -curve, parametrised as $t \mapsto (x(t), y(t)) = (t, 0)$, this frame is

$$\cos(2\pi t)\partial_z + \sin(2\pi t)\cos a(-\partial_x + p\partial_y) = -\cos(2\pi t)\partial_r + \sin(2\pi t)\partial_\theta.$$

Translated into Cartesian coordinates (u, v) on the D^2 -factor of the solid torus, the curve (or rather its projection to the D^2 -factor) becomes

$$(u(t), v(t)) = (\cos 2\pi(p+1)t, -\sin 2\pi(p+1)t),$$

and translating the frame into Cartesian coordinates as above, we obtain

$$\begin{aligned} & -\cos(2\pi t)(\cos(2\pi(p+1)t)\partial_u - \sin(2\pi(p+1)t)\partial_v) + \\ & \sin(2\pi t)(\cos(2\pi(p+1)t)\partial_v + \sin(2\pi(p+1)t)\partial_u) = \\ & -\cos(2\pi(p+2)t)\partial_u + \sin(2\pi(p+2)t)\partial_v. \end{aligned}$$

This formula defines the extension of the frame over the helicoidal annulus and the straight annulus inside the solid torus. Along the intersection of the straight annulus with the boundary of the solid torus, given again by $\{u = 1, v = 0\}$, and further on the annulus between $p\lambda = p(-1, p+1)$ and pL_1 , this frame extends as

$$\cos(2\pi(p+2)t)\partial_z - \sin(2\pi(p+2)t)X_2,$$

since at $(u, v) = (1, 0)$ the vector ∂_u is the outward normal $-\partial_z$, and ∂_v points in meridional direction, which is identified with $-X_2$.

This frame makes $p+2$ *negative* rotations with respect to the tangent direction X_2 of L_1 , which yields $\text{rot}_{\mathbb{Q}}(L_1) = (p+2)/p = 1 + 2/p$.

Since we may flip the orientations of L_0 and L_1 simultaneously, this gives us in total two realisations, with invariants

$$(\text{tb}_{\mathbb{Q}}(L_0), \text{rot}_{\mathbb{Q}}(L_0)) = \left(\frac{1}{p}, \pm \frac{2}{p}\right), \quad (\text{tb}_{\mathbb{Q}}(L_1), \text{rot}_{\mathbb{Q}}(L_1)) = \left(1 + \frac{1}{p}, \pm \left(1 + \frac{2}{p}\right)\right).$$

Remark 5.3. For $p = 1$, this accords with the case $(1, \pm 2)$ and $(2, \pm 3)$ discussed in [7, Section 7.4].

6. DETECTING EXCEPTIONAL LINKS

Before we turn to the Legendrian realisations of Legendrian Hopf links in $L(p, 1)$ in terms of contact surgery diagrams, we discuss how to establish that a given Hopf link is exceptional, and how to decide whether the individual components are loose or exceptional.

First one needs to verify that the contact structure given by the surgery diagram is overtwisted. If the d_3 -invariant differs from that of any of the tight structure (see Remark 4.1), this is obvious. If the d_3 -invariant *does* match that of a tight structure, overtwistedness can be shown by exhibiting a Legendrian knot in the surgered manifold that violates the Bennequin inequality [1, Theorem 1] for Legendrian knots in tight contact 3-manifolds. In all our examples, one of L_0 or L_1 will have this property. Alternatively, one can appeal to the classification of Legendrian rational unknots in $L(p, 1)$ with a tight contact structure [6, Theorem 7.1 (a)]. If the invariants of L_0 or L_1 do not match those listed there (in particular, $\text{tb}_{\mathbb{Q}}(L) = \mathfrak{t} + 1/p$ with \mathfrak{t} a negative integer), then the contact structure must be overtwisted. Again, this covers all cases (b)–(e).

Secondly, we need to establish that the contact structure on the link complement $L(p, 1) \setminus (L_0 \sqcup L_1)$ is tight. The method we use is to perform contact surgeries on L_0 and L_1 , perhaps also on Legendrian push-offs of these knots, such that the resulting contact manifold is tight. If there had been an overtwisted disc in the complement of $L_0 \sqcup L_1$, this would persist after the surgery.

Here we rely on the cancellation lemma from [3], cf. [5, Proposition 6.4.5], which says that a contact (-1) -surgery and a contact $(+1)$ -surgery along a Legendrian knot and its Legendrian push-off, respectively, cancel each other. For instance, if by contact (-1) -surgeries on L_0 and L_1 we can cancel all contact $(+1)$ -surgeries in the surgery diagram, and thus obtain a Stein fillable and hence tight contact 3-manifold, the Legendrian Hopf link will have been exceptional.

To determine whether one of the link components is loose, we sometimes rely on the classification of exceptional rational unknots in $L(p, 1)$ given in [6, Theorem 7.1]:

Theorem 6.1. *Up to coarse equivalence, the exceptional rational unknots in $L(p, 1)$ are classified by their classical invariants $\mathbf{tb}_{\mathbb{Q}}$ and $\mathbf{rot}_{\mathbb{Q}}$. The possible values of $\mathbf{tb}_{\mathbb{Q}}$ are $\mathbf{t} + 1/p$ with $\mathbf{t} \in \mathbb{N}_0$. For $\mathbf{t} = 0$, there is a single exceptional knot, with $\mathbf{rot}_{\mathbb{Q}} = 0$. For $\mathbf{t} = 1$, there are $p + 1$ exceptional knots, with*

$$\mathbf{rot}_{\mathbb{Q}} \in \left\{ -1, -1 + \frac{2}{p}, -1 + \frac{4}{p}, \dots, -1 + \frac{2p}{p} \right\}.$$

For $\mathbf{t} \geq 2$, there are $2p$ exceptional knots, with

$$\mathbf{rot}_{\mathbb{Q}} \in \left\{ \pm \left(\mathbf{t} - 2 + \frac{2}{p} \right), \pm \left(\mathbf{t} - 2 + \frac{4}{p} \right), \dots, \pm \left(\mathbf{t} - 2 + \frac{2p}{p} \right) \right\}.$$

In a few cases, the invariants of one link component equal those realised by an exceptional rational unknot, but we detect looseness by computing the d_3 -invariant and observing, again comparing with [6], that it does not match that of an exceptional realisation.

7. EXCEPTIONAL HOPF LINKS

In this section we find exceptional Legendrian realisations of the Hopf link, except case (c1)—which is covered by Section 5—, in contact surgery diagrams for $L(p, 1)$. This completes the proof of Theorem 1.2.

7.1. Kirby diagrams. We begin with some examples of Kirby diagrams of the Hopf link that will be relevant in several cases of this classification. The proof of the following lemma is given by the Kirby moves in the corresponding diagrams.

Lemma 7.1. *(i) The oriented link $L_0 \sqcup L_1$ in the surgery diagram shown in the first line of Figure 3 is a positive or negative Hopf link in $L(p, 1)$, depending on k being even or odd. The same is true for the links shown in the first line of Figure 5 and 7, respectively.*

(ii) The oriented link $L_0 \sqcup L_1$ shown in Figure 4 is a positive Hopf link in $L(p, 1)$.

(iii) The oriented link $L_0 \sqcup L_1$ in the first line of Figure 6 is a positive or negative Hopf link depending on k_0 and k_1 having the same parity or not. \square

7.2. Legendrian realisations.

7.2.1. Case (b). The $|\mathbf{t}_1 - 1|$ realisations with $\mathbf{t}_0 = 0$ and $\mathbf{t}_1 \leq 0$ are shown in Figure 8. Here k and ℓ denote the number of stabilisations, with $k + \ell = -\mathbf{t}_1$, so that $\mathbf{tb}_1 = \mathbf{t}_1 - 1$.

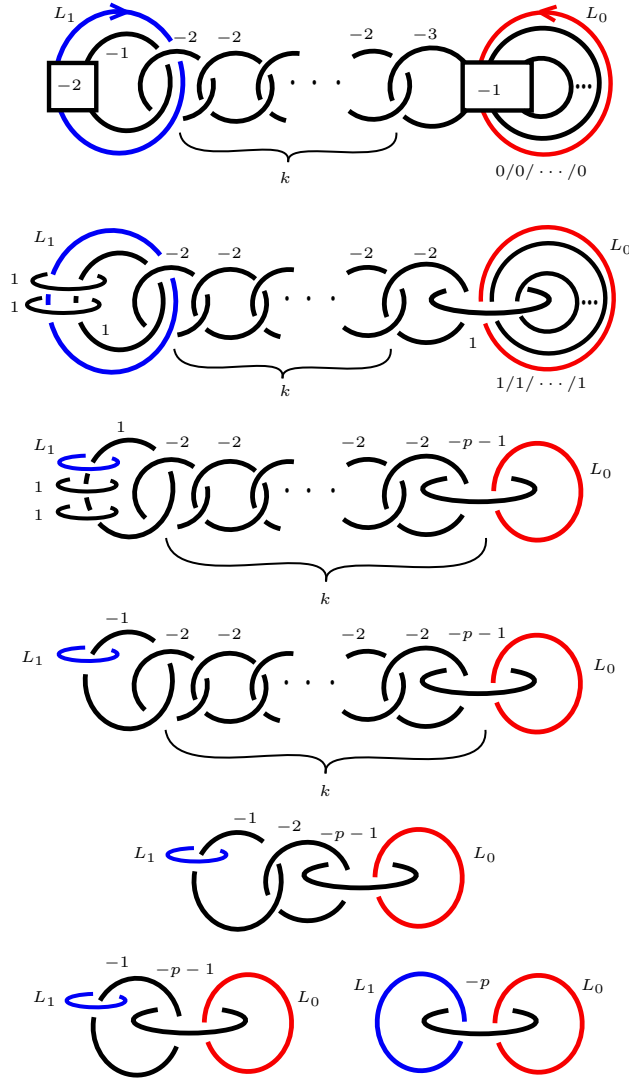


FIGURE 3. Kirby moves for (c3).

The linking matrix M of the surgery diagram is the $((p+1) \times (p+1))$ -matrix

$$\begin{pmatrix} 0 & -1 & -1 & \cdots & -1 \\ -1 & 0 & -1 & \cdots & -1 \\ -1 & -1 & 0 & \cdots & -1 \\ \vdots & \vdots & \vdots & \ddots & \vdots \\ -1 & -1 & -1 & \cdots & 0 \end{pmatrix}.$$

The determinant of this matrix is $\det M = -p$. The extended linking matrix for L_i , $i = 0, 1$, is the $((p+2) \times (p+2))$ -matrix built in the same fashion as M , so that $\det(M_i) = -p - 1$.

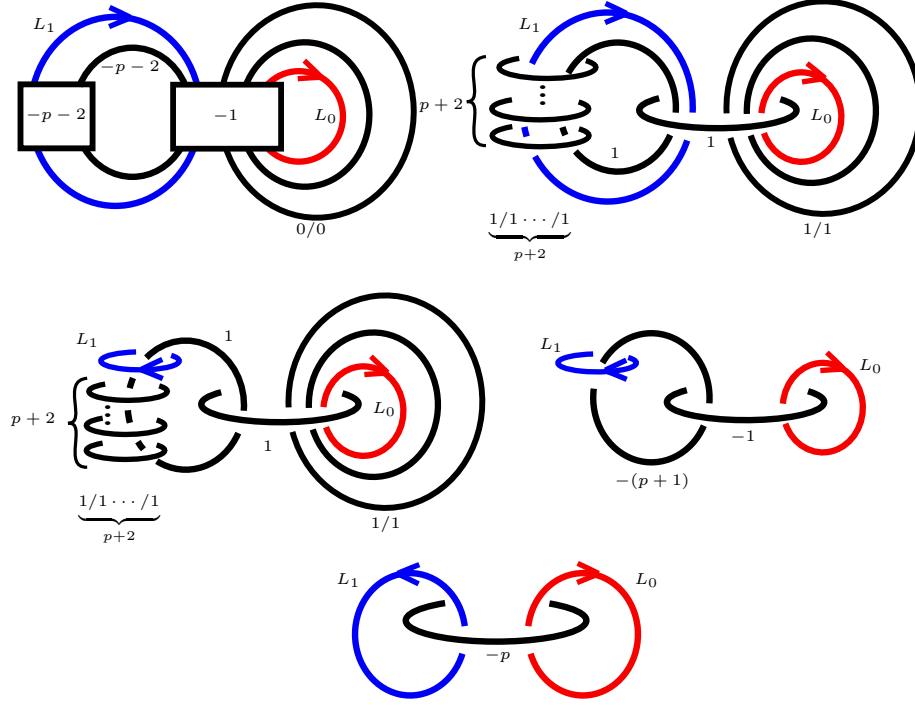


FIGURE 4. Kirby moves for (d1).

It follows that

$$\text{tb}_{\mathbb{Q}}(L_0) = -1 + \frac{p+1}{p} = \frac{1}{p}$$

and

$$\text{tb}_{\mathbb{Q}}(L_1) = \mathfrak{t}_1 - 1 + \frac{p+1}{p} = \mathfrak{t}_1 + \frac{1}{p}.$$

Since $\underline{\text{rot}} = \underline{0}$, we get $\text{rot}_{\mathbb{Q}}(L_0) = 0$ and

$$\text{rot}_{\mathbb{Q}}(L_1) \in \{\mathfrak{t}_1, \mathfrak{t}_1 + 2, \dots, -\mathfrak{t}_1 - 2, -\mathfrak{t}_1\}.$$

For the calculation of d_3 , we observe that $c^2 = 0$, $\chi = p + 2$, and $\sigma = p - 1$. Thus,

$$d_3 = \frac{1}{4}(0 - 2(p + 2) - 3(p - 1)) + p + 1 = \frac{1}{4}(-5p - 1) + p + 1 = \frac{3 - p}{4}.$$

By Theorem 6.1, there are no exceptional realisations of a rational unknot in $L(p, 1)$ with $\text{tb}_{\mathbb{Q}}$ equal to that of L_1 , so L_1 is loose. The component L_0 is exceptional, as can be seen by performing surgery on it. A contact $(-\frac{1}{p+2})$ -surgery on L_0 has the same effect as taking $p + 2$ Legendrian push-offs of L_0 and doing a (-1) -surgery on each of them. This cancels the $(+1)$ -surgeries in the diagram and hence produces a tight contact 3-manifold.

7.2.2. Case (c2). In this case we have exactly three Legendrian realisations. The left-hand side of Figure 9, where the rational rotation numbers of L_0 and L_1 will be shown to be non-zero, gives two realisations (one with L_0, L_1 oriented as shown,

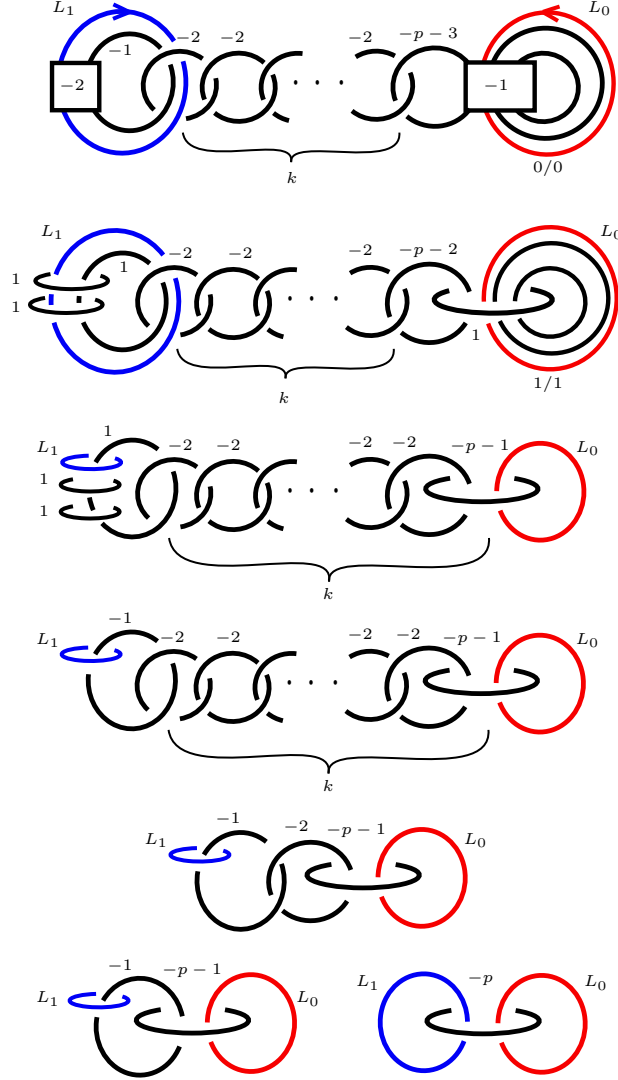


FIGURE 5. Kirby moves for (d2).

the second with orientations flipped simultaneously. The right-hand side, where the rotation numbers are zero, gives the third one.

We begin with the left-hand side. The linking matrix for the surgery diagram, ordering the surgery knots from top to bottom, and with all surgery knots oriented clockwise, is the $((p+3) \times (p+3))$ -matrix

$$M = \begin{pmatrix} -2 & -1 & -1 & \cdots & -1 \\ -1 & 0 & -1 & \cdots & -1 \\ -1 & -1 & 0 & \cdots & -1 \\ \vdots & \vdots & \vdots & \ddots & \vdots \\ -1 & -1 & -1 & \cdots & 0 \end{pmatrix},$$

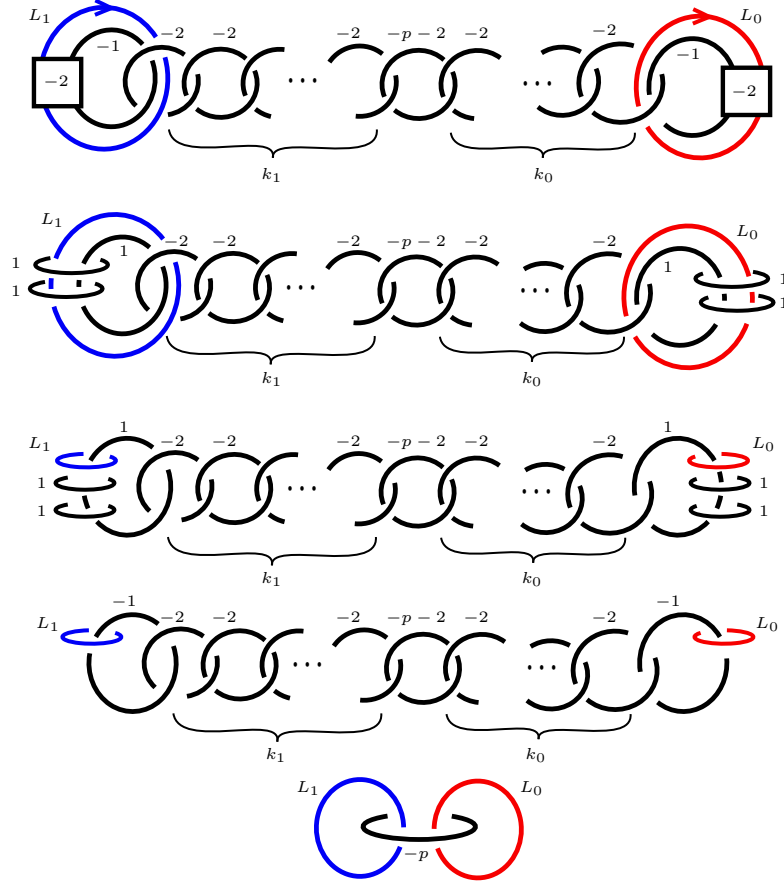


FIGURE 6. Kirby moves for (d3).

with $\det M = p$.

The extended linking matrices for L_0 and L_1 are

$$M_0 = \left(\begin{array}{c|cccc} 0 & -1 & -1 & \cdots & -1 \\ \hline -1 & & & & \\ -1 & & M & & \\ \vdots & & & & \\ -1 & & & & \end{array} \right),$$

with $\det M_0 = 1 + p$, and

$$M_1 = \left(\begin{array}{c|cccc} 0 & 3 & 1 & \cdots & 1 \\ \hline 3 & & & & \\ 1 & & M & & \\ \vdots & & & & \\ 1 & & & & \end{array} \right),$$

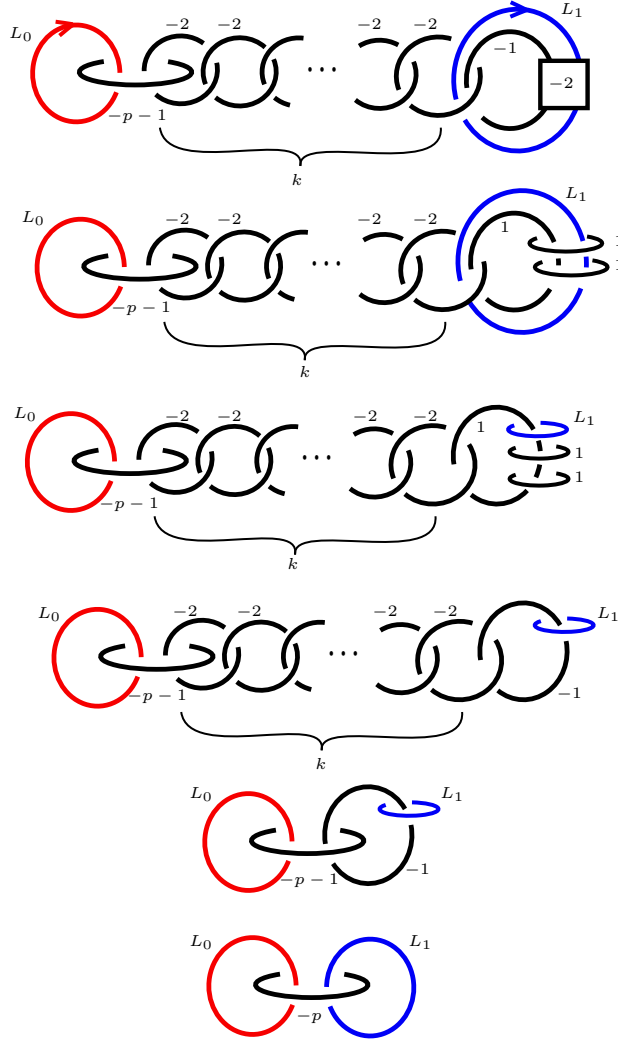


FIGURE 7. Kirby moves for (e2).

with $\det M_1 = 1 + 5p$. This yields

$$\text{tb}_{\mathbb{Q}}(L_0) = -1 + \frac{1+p}{p} = \frac{1}{p} \quad \text{and} \quad \text{tb}_{\mathbb{Q}}(L_1) = -3 + \frac{1+5p}{p} = 2 + \frac{1}{p},$$

so we are indeed in the case $(\mathfrak{t}_0, \mathfrak{t}_1) = (0, 2)$. Further,

$$\underline{\text{rot}} = (2, \underbrace{0, 0, \dots, 0}_{p+2}), \quad \underline{\mathbf{k}}_0 = (-1, \underbrace{-1, \dots, -1}_{p+2}), \quad \underline{\mathbf{k}}_1 = (3, \underbrace{1, \dots, 1}_{p+2}).$$

A simple calculation gives

$$M^{-1}\underline{\mathbf{k}}_0 = (-1/p, 1/p, \dots, 1/p) \quad \text{and} \quad M^{-1}\underline{\mathbf{k}}_1 = (-(2p+1)/p, 1/p, \dots, 1/p).$$

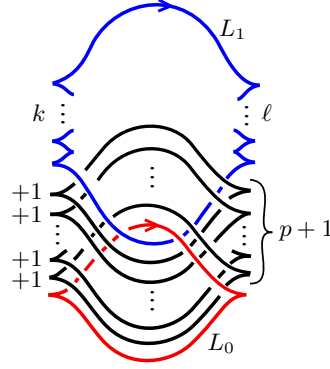
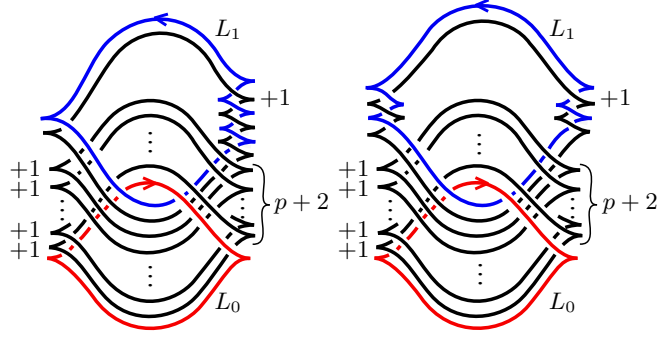
FIGURE 8. $|\mathbf{t}_1 - 1|$ Legendrian realisations for case (b).

FIGURE 9. Three Legendrian realisations for case (c2).

Hence

$$\text{rot}_{\mathbb{Q}}(L_0) = 0 - 2 \cdot \frac{-1}{p} = \frac{2}{p} \quad \text{and} \quad \text{rot}_{\mathbb{Q}}(L_1) = -2 + 2 \cdot \frac{2p+1}{p} = 2 + \frac{2}{p}.$$

The second realisation is given by reversing the orientations of both L_0 and L_1 ; this changes the sign of the $\text{rot}_{\mathbb{Q}}(L_i)$ (as is best seen by also changing the orientations of the surgery curves, although the choice of orientation here does not matter).

For the diagram on the right, the calculation of $\text{tb}_{\mathbb{Q}}(L_i)$ does not change, but now we have $\underline{\text{rot}} = \underline{0}$ and $\text{rot}_1 = 0$, whence $\text{rot}_{\mathbb{Q}}(L_0) = \text{rot}_{\mathbb{Q}}(L_1) = 0$. This yields the third realisation.

For the calculation of the d_3 -invariant we observe that both diagrams in Figure 9 give $\sigma = p - 1$ and $\chi = p + 4$. The diagram on the right has $\underline{\text{rot}} = \underline{0}$, which yields $d_3 = (7 - p)/4$. For the diagram on the left, the solution \mathbf{x} of $M\mathbf{x} = \underline{\text{rot}}$ is $\mathbf{x} = (-2 - 2/p, 2/p, \dots, 2/p)^t$. Then $c^2 = \langle \mathbf{x}, \underline{\text{rot}} \rangle = -2(2 + 2/p)$ and $d_3 = (3p - p^2 - 4)/4p$.

In either case, the contact structure is overtwisted by the observations in Section 6. A contact (-1) -surgery along L_1 and a contact $(-\frac{1}{p+2})$ -surgery along L_0 cancels all $(+1)$ -surgeries, so the link is exceptional. Both components are loose, since the classical invariants do not match those of Theorem 6.1.

\mathfrak{t}_0	$\text{rot}_{\mathbb{Q}}(L_0)$	\mathfrak{t}_1	$\text{rot}_{\mathbb{Q}}(L_1)$	d_3
0	0	> 2	$\pm(\mathfrak{t}_1 - 2)$	$\frac{7-p}{4}$
0	$\pm\frac{2}{p}$	> 2	$\pm(\mathfrak{t}_1 + \frac{2}{p})$	$\frac{3p-p^2-4}{4p}$

TABLE 1. Invariants for case (c3).

Case (c3). Two of the four Legendrian realisations in this case are shown in Figure 10, with L_0 and L_1 both oriented clockwise or counter-clockwise for k even, L_1 having the opposite orientation of L_0 for k odd; cf. Figure 3. The other two are obtained by flipping the shark with surgery coefficient -1 . The invariants are shown in Table 1. We omit the calculations of the invariants in this and the remaining cases. The arithmetic is lengthy but not inspiring; the detailed calculations are available from the authors upon request.

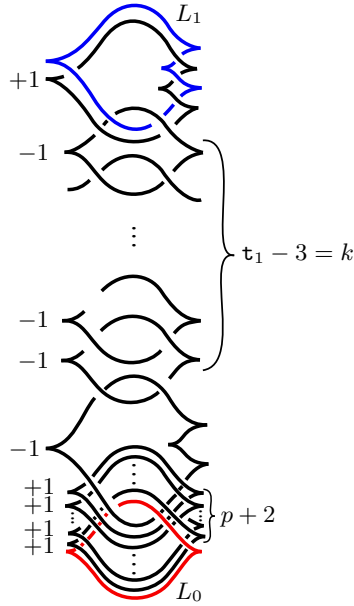


FIGURE 10. Legendrian realisations for case (c3).

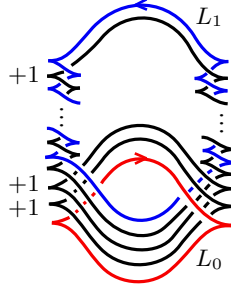
The contact structure is overtwisted, because we have rational unknots with $\mathfrak{t}_i \geq 0$. A contact (-1) -surgery on L_1 and a contact $(-\frac{1}{p+2})$ -surgery on L_0 will cancel all contact $(+1)$ -surgeries, so the link is exceptional.

Except for $(\mathfrak{t}_0, \text{rot}_{\mathbb{Q}}(L_0)) = (0, 0)$, the invariants of L_0 and L_1 are not realised by exceptional rational unknots, see Theorem 6.1 or, for a better overview, [6, Table 2]; hence these knots are loose. So is L_0 in the first line of Table 1, since the value of the d_3 -invariant does not match that of an exceptional realisation; again see [6, Table 2]. This is the first instance where we need the d_3 -invariant to detect looseness.

\mathfrak{t}_0	$\text{rot}_{\mathbb{Q}}(L_0)$	\mathfrak{t}_1	$\text{rot}_{\mathbb{Q}}(L_1)$	d_3
1	$\pm \frac{1-\mathfrak{r}}{p}$	> 1	$\pm(\mathfrak{t}_1 - 1 + \frac{1-\mathfrak{r}}{p})$	$\frac{7p-1+2\mathfrak{r}-\mathfrak{r}^2}{4p}$

TABLE 2. Invariants for case (d2).

7.2.3. *Case (d1).* The $p + 3$ Legendrian realisations with invariants as listed in Theorem 1.2 are shown in Figure 11. The surgery knot of which L_1 is a push-off is a $(p + 2)$ -fold stabilisation of the standard Legendrian unknot (compare with the topological surgery framing in Figure 4); placing the stabilisations left or right gives the $p + 3$ choices. Flipping the orientations of both L_0 and L_1 has the same effect as exchanging the number of stabilisations on the left- and right-hand side, so this does not give any new choices.

FIGURE 11. $p + 3$ Legendrian realisations for case (d1).

The argument for the link being exceptional is as in the preceding case. According to [6, Table 2], the classical invariants are realised by exceptional rational unknots, but only in the overtwisted contact structure with $d_3 = (3p - \mathfrak{r}^2)/4p$, so the link components here are loose.

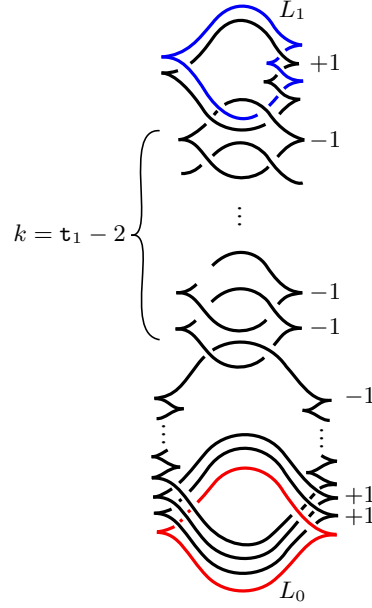
7.2.4. *Case (d2).* The $2(p + 2)$ Legendrian realisations are shown in Figure 12, with L_0, L_1 given the same orientation for k even, the opposite, for k odd. The factor 2 comes from simultaneously exchanging the orientations of L_0 and L_1 . The factor $p + 2$ comes from the placement of $p + 1$ stabilisations on the surgery knot near the bottom of the diagram (compare with Figure 5). We write

$$\mathfrak{r} \in \{-p - 1, -p + 1, \dots, p - 1, p + 1\}$$

for the $p + 2$ possible rotation numbers of this surgery knot. The invariants are listed in Table 2. The remaining arguments are as before.

7.2.5. *Case (d3).* The $4(p + 1)$ Legendrian realisations are shown in Figure 13. For k_0, k_1 of equal parity, we give L_0 and L_1 the same orientation; for k_0, k_1 of opposite parity, the opposite orientation. A factor 2 comes from exchanging the orientations simultaneously, a factor 2 from the two diagrams, and a factor $p + 1$ from placing p stabilisations left or right on the surgery knot at the centre of each diagram, cf. Figure 6. The rotation number of this surgery knot is denoted by

$$\mathfrak{r} \in \{-p, -p + 2, \dots, p - 2, p\}.$$

FIGURE 12. $2(p+2)$ Legendrian realisations for case (d2).

\mathfrak{t}_0	$\text{rot}_{\mathbb{Q}}(L_0)$	\mathfrak{t}_1	$\text{rot}_{\mathbb{Q}}(L_1)$	d_3
> 1	$\pm(\mathfrak{t}_0 - 1 + \frac{2-\mathfrak{r}}{p})$	> 1	$\pm(\mathfrak{t}_1 - 1 + \frac{2-\mathfrak{r}}{p})$	$\frac{7p-4+4\mathfrak{r}-\mathfrak{r}^2}{4p}$
> 1	$\pm(\mathfrak{t}_0 - 1 + \frac{\mathfrak{r}}{p})$	> 1	$\mp(\mathfrak{t}_1 - 1 - \frac{\mathfrak{r}}{p})$	$\frac{7p-\mathfrak{r}^2}{4p}$

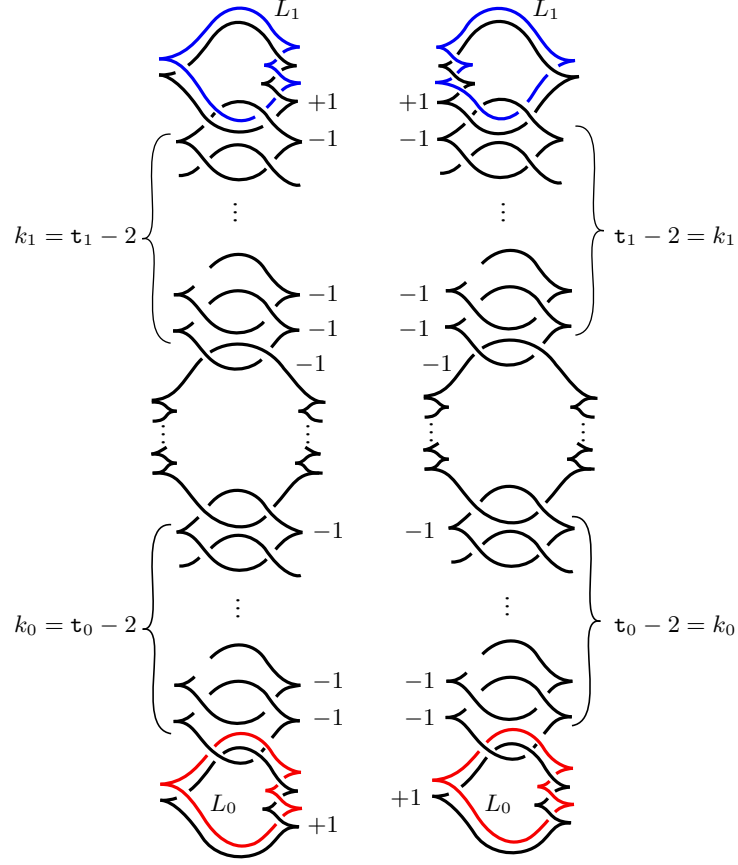
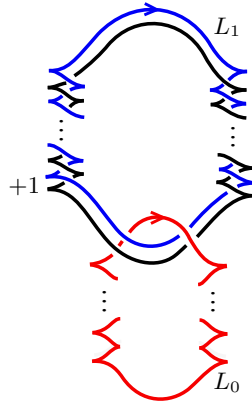
TABLE 3. Invariants for case (d3).

The invariants are shown in Table 3. As before, suitable contact surgeries along L_0, L_1 and comparison with [6] show that the link is exceptional and the components loose.

7.2.6. Case (e1). Figure 14 shows $|\mathfrak{tb}_0|(p+1)$ Legendrian realisations. Placing the $|\mathfrak{tb}_0| - 1$ stabilisations left or right gives $|\mathfrak{tb}_0|$ choices. The surgery knot is the standard Legendrian unknot with p stabilisations, which gives $p+1$ choices. Flipping the orientations of L_0, L_1 simultaneously is the same as flipping the whole diagram (and the left/right stabilisations), so this does not give any additional realisations. Write

$$\mathfrak{r} \in \{-p, -p+2, \dots, p-2, p\}$$

for the rotation number of the surgery knot. A straightforward calculation then gives $\mathfrak{t}_0 = \mathfrak{tb}_0$ (and hence the right number of realisations) and the other classical invariants as listed in Theorem 1.2, with $\mathfrak{r}_0 := \text{rot}_{\mathbb{Q}}(L_0)$. The d_3 -invariant takes the value $(3p - \mathfrak{r}^2)/4p$. Since $\mathfrak{t}_1 > 0$, the contact structure is overtwisted. A contact (-1) -surgery on L_1 gives (S^3, ξ_{st}) , so L_1 is exceptional. On the other hand, L_0 must be loose, since $\mathfrak{t}_0 < 0$.

FIGURE 13. $4(p+1)$ Legendrian realisations for case (d3).FIGURE 14. $|t_0|(p+1)$ Legendrian realisations for case (e1).

7.2.7. *Case (e2).* The $2|t_0|p$ realisations for this case are shown in Figure 15, with L_0 and L_1 both oriented clockwise or counter-clockwise for k odd, L_1 having the

opposite orientation of L_0 for k even; cf. Figure 7. Here L_0 is an unknot with $\mathbf{tb}_0 < 0$ (which will again turn out to equal \mathbf{t}_0); this gives us $|\mathbf{t}_0|$ choices distinguished by

$$\mathbf{r}_0 := \mathbf{rot}_0 \in \{\mathbf{t}_0 + 1, \mathbf{t}_0 + 3, \dots, -\mathbf{t}_0 - 3, -\mathbf{t}_0 - 1\}.$$

The topmost surgery knot has Thurston–Bennequin invariant $-p$; this gives us p choices distinguished by the rotation number

$$\mathbf{r} \in \{-p + 1, -p + 3, \dots, p - 3, p - 1\}.$$

The factor 2 in the number of choices comes from simultaneously flipping the orientations of L_0 and L_1 .

One then computes that

$$\mathbf{rot}_{\mathbb{Q}}(L_0) = \pm \left(\mathbf{r}_0 + \frac{\mathbf{r} + 1}{p} \right), \quad \mathbf{rot}_{\mathbb{Q}}(L_1) = \pm \left(\mathbf{t}_1 - 1 + \frac{\mathbf{r} + 1}{p} \right),$$

and

$$d_3 = \frac{1}{4} \left(3 + \frac{2\mathbf{r} - \mathbf{r}^2 - 1}{p} \right).$$

The argument for showing that L_0 is loose, and L_1 exceptional, is as in case (e1).

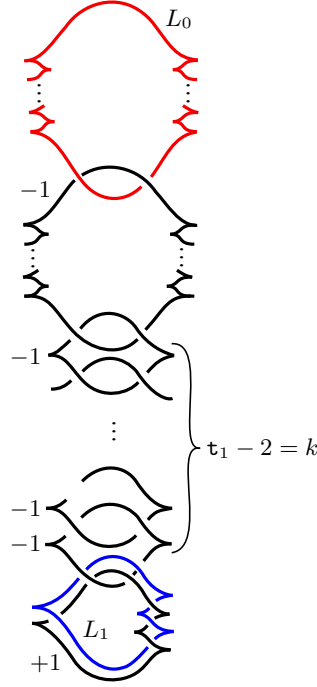


FIGURE 15. $2|\mathbf{t}_0|p$ Legendrian realisations for case (e2).

REFERENCES

- [1] K. BAKER AND J. ETNYRE, Rational linking and contact geometry, *Perspectives in Analysis, Geometry, and Topology*, Progr. Math. **296** (Birkhäuser Verlag, Basel, 2012), 19–37.
- [2] R. CHATTERJEE AND M. KEGEL, Contact surgery numbers of $\Sigma(2, 3, 11)$ and $L(4m + 3, 4)$, [arXiv:2404.18177](#).

- [3] F. DING AND H. GEIGES, A Legendrian surgery presentation of contact 3-manifolds, *Math. Proc. Cambridge Philos. Soc.* **136** (2004), 583–598.
- [4] F. DING, H. GEIGES AND A. I. STIPSICZ, Surgery diagrams for contact 3-manifolds, *Turkish J. Math.* **28** (2004), 41–74.
- [5] H. GEIGES, *An Introduction to Contact Topology*, Cambridge Stud. Adv. Math. **109** (Cambridge University Press, Cambridge, 2008).
- [6] H. GEIGES AND S. ONARAN, Legendrian rational unknots in lens spaces, *J. Symplectic Geom.* **13** (2015), 17–50.
- [7] H. GEIGES AND S. ONARAN, Legendrian Hopf links, *Quart. J. Math.* **71** (2020), 1419–1459.
- [8] E. GIROUX, Structures de contact en dimension trois et bifurcations des feuilletages de surfaces, *Invent. Math.* **141** (2000), 615–689.
- [9] K. HONDA, On the classification of tight contact structures I, *Geom. Topol.* **4** (2000), 309–368; erratum: *Geom. Topol.* **5** (2001), 925–938.
- [10] E. LERMAN, Contact cuts, *Israel J. Math.* **124** (2001), 77–92.

MATHEMATISCHES INSTITUT, UNIVERSITÄT ZU KÖLN, WEYERTAL 86–90, 50931 KÖLN, GERMANY

Email address: `rchatt@math.uni-koeln.de`

Email address: `geiges@math.uni-koeln.de`

DEPARTMENT OF MATHEMATICS, HACETTEPE UNIVERSITY, 06800 BEYTEPE-ANKARA, TURKEY

Email address: `sonaran@hacettepe.edu.tr`